



UNIVERSITY  
OF TRENTO

---

**DIPARTIMENTO DI INGEGNERIA E SCIENZA DELL'INFORMAZIONE**

---

38123 Povo – Trento (Italy), Via Sommarive 14  
<http://www.disi.unitn.it>

DETECTION OF MULTIPLE DEFECTS IN INDUSTRIAL  
PRODUCTS BY MEANS OF A NON-DESTRUCTIVE MICROWAVE  
APPROACH

M. Benedetti, M. Donelli, M. Pastorino, A. Rosani, and A. Massa

January 2011

Technical Report # DISI-11-246



# DETECTION OF MULTIPLE DEFECTS IN INDUSTRIAL PRODUCTS BY MEANS OF A NON-DESTRUCTIVE MICROWAVE APPROACH

M. Benedetti<sup>(1)</sup>, M. Donelli<sup>(1)</sup>, M. Pastorino<sup>(2)</sup>, A. Rosani<sup>(1)</sup>, and A. Massa<sup>(1)</sup>

<sup>(1)</sup>*Department of Information and Communication Technology,  
University of Trento, Via Sommarive 14, 38050 Trento, Italy*

*Email: andrea.massa@ing.unitn.it, {massimo.donelli, andrea.rosani, manuel.benedetti}@dit.unitn.it*

<sup>(2)</sup>*Department of Biophysical and Electronic Engineering,  
University of Genoa, Via Opera Pia 11a, 16145 Genoa, Italy  
E-mail: pastorino@dibe.unige.it*

## ABSTRACT

This paper proposes an approach for the detection of multiple defects inside a known host medium. Two innovative GA-based techniques are developed by using different strategies for the minimization of a suitably defined cost function. The first implementation is based on a set of parallel GA-based optimization sub-processes, whereas the other consists of a single process based on a variable length coding of the GA chromosomes. A set of representative test cases is analyzed for assessing potentialities and current limitations of the proposed strategy.

## 1. INTRODUCTION

In the framework of inspection techniques, the non-destructive evaluation and testing (NDE/NDT) are mandatory in many industrial processes. Within the context of microwave methodologies, state-of-the-art techniques consider interrogating microwaves as direct diagnostic non-invasive instruments [1]-[3]. A further advance is represented by the inverse scattering approaches [4][5], where a reconstruction of the electromagnetic properties in the whole region under test is carried out processing the e.m. signals scattered from the structure under test. Unfortunately, these techniques are affected by the non-linearity (i.e., the presence of local minima) and the ill-positioning of the arising mathematical problem. Moreover, the wavelength of the probing microwave signal actually limits the achievable spatial resolution, requiring an high computational cost for allowing a detailed reconstruction of the scenario under test. Therefore, inversion techniques are currently far from a realistic application. However, the feasibility of the detection of a simple unknown scatterer inside a known host medium has been positively addressed in [6] and [7] by recurring to the exploitation of the a-priori information on the problem at hand. In order to deal with more complex and realistic scenarios (i.e., multiple defects), this paper presents two GA-based strategies for solving the problem of the detection of multiple defective regions inside a known dielectric host-medium. By assuming that the knowledge of the unperturbed geometry of the region under test is a-priori available, the cracks are described in terms of a set of essential parameters and coded through multiple-length chromosomes. As far as the difference between the proposed implementations is concerned, the former strategy is based on a set of parallel detection processes, while the other is based on a single process.

The paper is organized as follows. A short mathematical formulation (Sec. 2) illustrates the e.m. scenario and the arising inverse scattering relationship. Successively the key-issues concerned with two different GA-based solution procedures are presented. Finally (Sec. 3), a numerical assessment is carried out through the reconstruction results from a set of representative synthetic test cases.

## 2. MATHEMATICAL FORMULATION

Under the assumption of two-dimensional geometry, let us consider a square host area  $H$  lying in a free-space  $(\epsilon_0, \mu_0)$  background and occupied by a known host medium characterized by an object function  $\tau_H(x, y) = \epsilon_H - 1 - j \frac{\sigma_H}{2\omega\epsilon_0}$ ,  $\epsilon_H$  and  $\sigma_H$  being the relative permittivity and conductivity, respectively. Let us assume that a set of  $C$  defects  $D_i$ , ( $i=1, \dots, C$ ), characterized by unknown geometric and electromagnetic properties belongs to  $H$ . A set of  $V$  electromagnetic TM plane waves  $\underline{E}_{inc}^v(x, y) = E_{inc}^v(x, y)\hat{z}$  illuminate such a scenario, inducing an electromagnetic field given by

$$E_{tot}^v(x, y) = E_{inc}^v(x, y) + \iint_H \tau(x', y') E_{tot(c)}^v(x', y') G_0(x', y' / x, y) dx' dy' \quad (1)$$

where  $G_0$  is the free-space Green's function and  $\tau(x, y) = \varepsilon(x, y) - 1 - j \frac{\sigma(x, y)}{2\pi\epsilon_0}$ ,  $f$  being the working frequency. By assuming that in each region  $D_i$  a differential equivalent current density radiates in an inhomogeneous medium, equation (1) can be rewritten as follows [8]

$$E_{tot}^v(x, y) = E_{inc(cf)}^v(x, y) + \sum_{i=1}^C \iint_{D_i} \tau_{D_i}(x', y') E_{tot(cf),i}^v(x', y') G_1(x', y' / x, y) dx' dy' \quad (2)$$

where  $E_{inc(cf)}^v(x, y)$  is the total electric field in the scenario under test without the defect, namely

$$E_{inc(cf)}^v(x, y) = E_{inc}^v(x, y) + \iint_H \tau_H(x', y') E_{tot(cf)}^v(x', y') G_0(x', y' / x, y) dx' dy' \quad (3)$$

and  $G_1$  is the inhomogeneous Green's function. In particular, the second term in the right side of (2) provides the electromagnetic field induced by the  $C$  differential object function  $\tau_{D_i}(x, y) = \tau(x, y) - \left\{ \varepsilon_H(x, y) - 1 - j \frac{\sigma_H(x, y)}{2\pi\epsilon_0} \right\}$ ,  $(x, y) \in D_i$ , with  $i = 1, \dots, C$ .

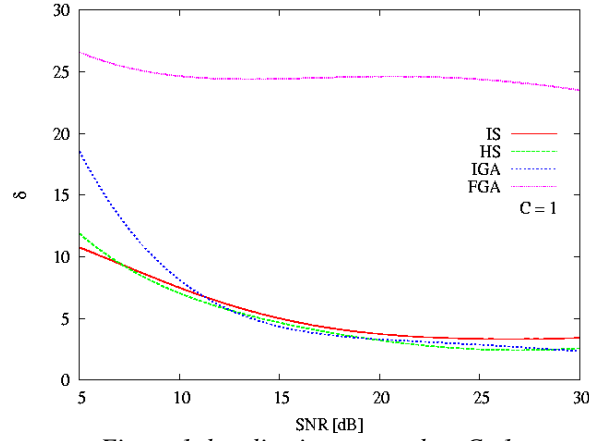


Figure 1, localization error when  $C=1$

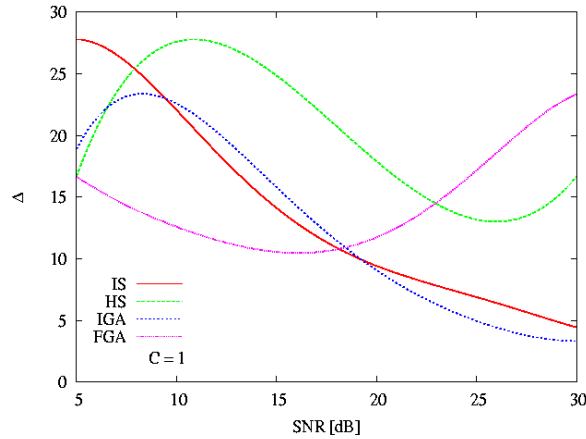


Figure 2, area error when  $C=1$

In order to numerically solve these equations, the region  $H$  is partitioned in  $N$  sub-domains according to the Richmond's method [9]. Therefore, the Green's inhomogeneous operator  $G_1$  can be discretized and stored in a  $N \times N$  matrix  $[G_1]$ . Moreover, let us indicate with  $P_i$  the number of pixel occupied by the defect  $D_i$ ; thus, (2) turns out to be expressed in matrix form as follows

$$[E_{tot}^v] = [E_{inc(cf)}^v] + [G_{1,i}] [\tau_{D_i}] [E_{tot(c),i}^v] \quad (3)$$

where

- $[E_{tot}^v]$  and  $[E_{inc(cf)}^v]$  are  $N \times I$  vectors, whose  $n$ th element are  $E_{tot}^v(x_n, y_n)$  and  $E_{inc(cf)}^v(x_n, y_n)$ , respectively, being  $(x_n, y_n) \in H$ ;
- $[E_{tot(c),i}^v]$  is a  $P_i \times I$  matrix whose  $p$ th element is  $E_{tot(c),i}^v(x_{p_i}, y_{p_i})$ , with  $p_i = 1, \dots, P_i$  and  $i = 1, \dots, C$ ;
- $[\tau_{D_i}]$  is a  $P_i \times P_i$  diagonal matrix are the values of the object function  $\tau_{D_i}$  in the  $P_i$  pixels of  $D_i$ ;
- $[G_{1,i}]$  is the  $i$ th inhomogeneous space Green's matrix of size  $N \times P_i$ , computed by selecting the  $P_i$  columns of  $[G_1]$  related to the position  $p_i$  ( $p_i = 1, \dots, P_i$ ) of the pixels of  $D_i$ .

Instead of describing each defect  $D_i$  through a set of pixel values of the contrast function, let us parameterize the  $i$ th defect by means of a set of geometric features. In particular, the center of the defective shape  $(x_i, y_i)$ , its length  $L_i$ , side  $W_i$  and orientation  $\theta_i$ . Therefore, the entries of  $[\tau_{D_i}]$  turns out to be given by:

$$\tau_{D_i}(x_n, y_n) = \begin{cases} \tau_{D_i} & \text{if } X \in \left[-\frac{L_i}{2}, \frac{L_i}{2}\right] \text{ and } Y \in \left[-\frac{W_i}{2}, \frac{W_i}{2}\right] \\ 0 & \text{otherwise} \end{cases} \quad (4)$$

where  $X = (x_n - x_i)\cos\theta_i + (y_n - y_i)\sin\theta_i$  and  $Y = (x_n - x_i)\sin\theta_i + (y_n - y_i)\cos\theta_i$ , with  $n = 1, \dots, P_i$ .

Since the problem unknowns are both the object function and the total electric field inside the  $C$  defective regions, the following set of parameters is looked for:

$$\chi = \{C; \Psi_i, i = 1, \dots, C; [E_{tot(c),i}^v], i = 1, \dots, C\} \quad (5)$$

where  $\Psi_i = [(x_i, y_i); L_i; W_i; \theta_i]$ .

In order to find the optimal solution  $\chi_{opt}$ , the problem at hand is recast as an optimization one. Starting from the information collected in the observation domain  $O$  [i.e., the total field with the defect  $E_{tot}^v(x_m, y_m)$  and without the defect  $E_{tot(cf)}^v(x_m, y_m)$ ,  $m = 1, \dots, M$ ] and in the investigation domain  $H$  [i.e.,  $E_{inc}^v(x_n, y_n)$ ,  $n = 1, \dots, N$ ], the following cost function has to be minimized through a suitable strategy

$$\Omega(\chi) = \alpha \left\{ \frac{\left\| [E_{tot}^v] - [E_{tot(cf)}^v] - \sum_{i=1}^C [G_{1,i}] [\tau_{D_i}] [E_{tot(i)}^v] \right\|_O^2}{\left\| [E_{tot}^v] - [E_{inc}^v] \right\|_O^2} \right\} + \beta \left\{ \frac{\left\| [E_{tot(cf)}^v] + [E_{tot}^v] - \sum_{i=1}^C [G_{1,i}] [\tau_{D_i}] [E_{tot(i)}^v] \right\|_H^2}{\left\| [E_{inc}^v] \right\|_H^2} \right\} \quad (6)$$

$\alpha$  and  $\beta$  being two regularization parameters. In the following sub-sections, two GA-based solution strategies will be described.

## 2.1. Hierarchical Strategy

Let us suppose that the number of defects lying in  $H$  is a fixed integer  $C_{max}$  lower than a fixed threshold ( $C_{max} < C$ ), then the hierarchical strategy (HS) performs the reconstruction through  $C_{max}$  parallel sub-processes, each aimed at determining the presence of a different number of defects, from 1 up to  $C_{max}$ . In the  $j$ th sub-process, a population of  $Q_j$  trial solutions coding a fixed number of crack  $j$  is considered:

$$\underline{\chi}_j = \{ \chi_{j,q}; q = 1, \dots, Q_j \} = \left\{ \left\{ C; \Psi_i, i = 1, \dots, j; [E_{tot(c),i}^v], i = 1, \dots, j \right\}; q = 1, \dots, Q_j \right\} \quad (7)$$

After a random initialization of  $\underline{\chi}_j^0$ , each  $j$ th process updates iteratively its  $Q_j$  trial solutions ( $\underline{\chi}_j^{k_j} \Rightarrow \underline{\chi}_j^{k_j+1}$ ,  $k_j$  being the iteration index) through a proper set of genetic operators, until a stopping criterion holds true ( $k_j < K_{max}$  or  $\Omega(\chi_{j,opt}) < \Omega_{th}$ ,

$$\chi_{j,opt} = \arg\left\{\min_{q=1,\dots,Q_j} \left[ \min_{k_j=1,\dots,K_{max}} \Omega(\chi_{j,q}^{k_j}) \right]\right\}.$$

Until the stopping criterion is satisfied, the set of operations performed in the  $j$ th processing can be summarized as follows:

- the iteration index is updated ( $k_j = k_j + 1$ );
- a set of genetic operators is applied to get the  $k_j$ th population [ $\underline{\chi}_j^{k_j} = \mathfrak{Z}(\underline{\chi}_j^{k_j-1})$ ];
- the best trial solution at the iteration  $k_j$  is found [ $\chi_{j,min}^{k_j} = \arg\left\{\min_{q=1,\dots,Q_j} \Omega(\chi_{j,q}^{k_j})\right\}$ ];
- the best individual of the  $j$ th process ( $\chi_{j,min} = \chi_{j,min}^{k_j}$ ) is updated if  $\Omega(\chi_{j,min}^{k_j}) < \Omega(\chi_{j,min})$ .

Thus, the solution of the reconstruction process is defined as  $\chi_{opt} = \arg\left\{\min_{q=1,\dots,Q_j} \Omega(\chi_{j,min})\right\}$ .

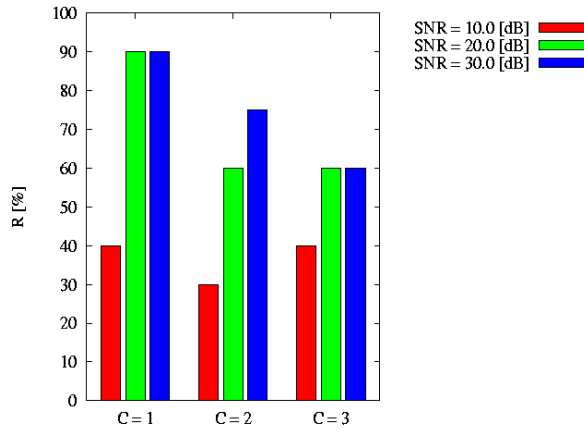


Figure 3, recall percentage R for HS

As far as the genetic operator  $\mathfrak{Z}(\cdot)$  is concerned, the *multicrack crossover*, *elitism*, *selection* and *mutation* are adopted [6][7]. Since each trial solution employs a *multicrack variable length hybrid coding* (i.e.,  $(x_i, y_i)$ ,  $L_i$ ,  $W_i$ ,  $\theta_i$  are supposed to be discrete binary encoded variables and for  $[E_{tot(c),i}^v]$  a real representation is used [6]), a single-point binary crossover  $\Phi_b$  is applied with probability  $\pi_b$  between two parents  $\underline{\chi}_{q_a}^{k_j}$  and  $\underline{\chi}_{q_b}^{k_j}$ , thus

$$\begin{aligned} \underline{\chi}_{q_a}^{k_j+1} &= \left\{ j; [\Psi_1]_{q_a}^{k_j}, \left[ (x_i, y_i)_{q_a}^{k_j} \right]_{cp}, (L_i)_{q_b}^{k_j}, (W_i)_{q_b}^{k_j}, (\theta_i)_{q_b}^{k_j}, \dots, [\Psi_j]_{q_b}^{k_j}, \right. \\ &\quad \left. [E_{tot(c),1}^v]_{q_a}^{k_j}, [E_{tot(c),2}^v]_{q_a}^{k_j+1}, \dots, [E_{tot(c),j}^v]_{q_b}^{k_j} \right\} \\ \underline{\chi}_{q_b}^{k_j+1} &= \left\{ j; [\Psi_1]_{q_b}^{k_j}, \left[ (x_i, y_i)_{q_b}^{k_j} \right]_{cp}, (L_i)_{q_a}^{k_j}, (W_i)_{q_a}^{k_j}, (\theta_i)_{q_a}^{k_j}, \dots, [\Psi_j]_{q_a}^{k_j}, \right. \\ &\quad \left. [E_{tot(c),1}^v]_{q_b}^{k_j}, [E_{tot(c),2}^v]_{q_b}^{k_j+1}, \dots, [E_{tot(c),j}^v]_{q_a}^{k_j} \right\} \end{aligned} \quad (8)$$

where  $cp$  indicates the crossover points, which is supposed to fall only on the boundary separating two genes. Concerning the computation of  $[E_{tot(c),2}^v]_{q_b}^{k_j+1}$  and  $[E_{tot(c),2}^v]_{q_b}^{k_j+1}$  in (8), the update equations described in [7] have been employed.

Moreover, if the binary crossover has not been applied, a double point crossover is performed according to the procedure detailed in [7] on the real part of the two individuals with probability  $\pi_d$ .

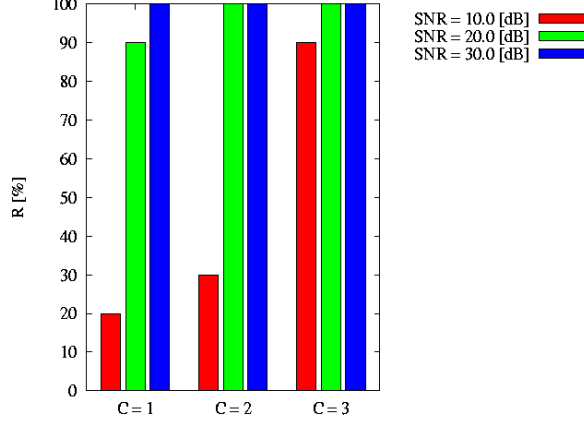


Figure 4, recall percentage  $R$  for IS

## 2.2. Integrated Strategy

Concerning the integrated strategy (IS), unlike the HS a single reconstruction process is carried out. Towards this aim, each population is composed by  $Q$  trial solutions coding a different number of cracks, from 1 up to  $C_{max}$

$$\underline{\chi} = \{\chi_q; q=1, \dots, Q_j\} = \left\{ \left( C_q; \Psi_i, i=1, \dots, j; [E_{tot(c),i}^v]_{i=1, \dots, C_q} \right); q=1, \dots, Q_j \right\} \quad (9)$$

$Q_j$  being a number between 1 and  $C_{max}$ . At the first iteration ( $k_j=0$ ), an initialization randomly generates the population  $\underline{\chi}^0$ . Then, until the same stopping criterion of HS is reached, the following operations are performed:

- the iteration index is updated ( $k=k+1$ );
- a population ( $\underline{\chi}_b^k$ ) of  $Q/2$  individuals coding the same number  $C_{opt}^{k-1}$  of defects as  $\underline{\chi}_{opt}^{k-1}$  is generated ( $\underline{\chi}_b^k = \Phi_b \{ \mathfrak{N}[\underline{\chi}_{opt}^{k-1}] \}$ );
- a population ( $\underline{\chi}_o^k$ ) of size  $Q/2$  is generated ( $\underline{\chi}_o^k = \wp[\underline{\chi}_{opt}^{k-1}]$ ), composed by  $C_{max}-1$  equally partitioned subsets, each of them coding the same number of cracks  $C_l$  ( $C_l=1, \dots, C_{max}$  but different from  $C_{opt}^{k-1}$ );
- standard *selection*, *mutation*, and *elitism* are applied on the trial solutions in order to get  $\underline{\chi}^k$ .

Consequently, the optimal solution turns out to be  $\chi_{min}^k = \arg\{\min_{q=1, \dots, Q} \Omega(\chi_q^k)\}$ .

As far as the operator  $\mathfrak{N}[\cdot]$  is concerned, the  $q$ th individual is given by:

$$\begin{aligned} \chi_{b,q}^{k-1} &= \mathfrak{N}\{\chi_{opt}^{k-1}\} = \\ &= \left\{ C_{opt}^{k-1}; \mathfrak{R}(\Psi_{opt,i}^{k-1}), i=1, \dots, C_{opt}^{k-1}; \mathfrak{R}([E_{tot,i}^v]_{opt}^{k-1}), i=1, \dots, C_{opt}^{k-1} \right\} \end{aligned} \quad (10)$$

where  $\mathfrak{R}(\cdot)$  is the random operator.

Furthermore, the operator  $\wp[\cdot]$  generates the population  $\underline{\chi}_o^k$  according to the following rules:

- if  $C_l < C_{opt}^{k-1}$ , then

$$\begin{aligned} \chi_{o,q}^k &= \\ &= \left\{ C_l; \Psi_i^k = \Psi_{opt,r}^{k-1}, i=1, \dots, C_l; [E_{tot,i}^v]^k = [E_{tot,s}^v]_{opt}^{k-1}, i=1, \dots, C_l \right\} \end{aligned} \quad (11)$$

- otherwise (i.e.,  $C_l > C_{opt}^{k-1}$ ), the trial solution is obtained by adding suitable genes to  $\chi_{opt}^{k-1}$ , randomly [ $\mathfrak{R}(\cdot)$ ] in the part concerned with the crack parameters, and from the field distribution of the unperturbed scenario in the remaining part.

### 3. RESULTS

In the following, a set of numerical results is discussed for assessing the effectiveness of the proposed GA-based implementations. Different scattering configuration have been considered and the robustness against noisy data has been evaluated, as well.

A new set of suitable error indexes has been defined extending those reported in [7]:

- the *multi-crack localization error*

$$\delta = \frac{1}{C} \sum_{c=1}^C \left\{ \left[ \sqrt{(\hat{x}_c - x_c)^2 - (\hat{y}_c - y_c)^2} / d_{\max} \right] \times 100 \right\} \quad (12)$$

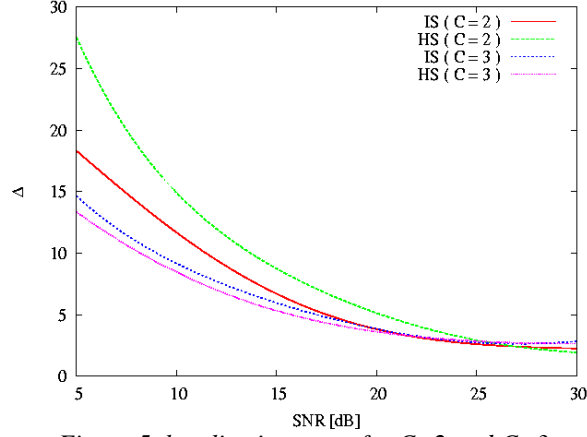


Figure 5, localization error for C=2 and C=3

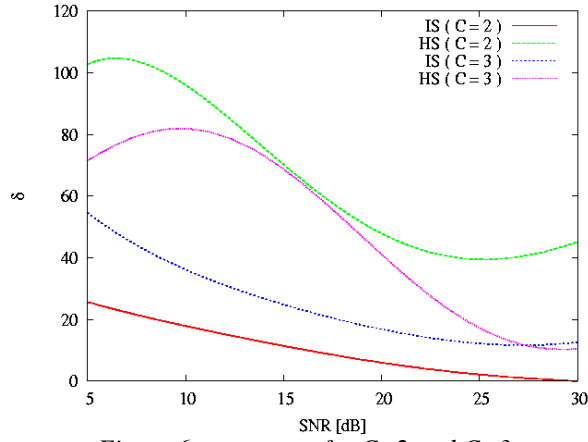


Figure 6, area error for C=2 and C=3

- the *multi-crack area error*

$$\Delta = \frac{1}{C} \sum_{c=1}^C \left\{ \left\| \hat{A}_c - A_c \right\| / A_c \right\} \times 100 \quad (13)$$

where the estimated quantities are denoted by  $\hat{\cdot}$ .

Moreover, the values of the precision recall index  $R$  have been determined in order to evaluate the accuracy in detecting multiple defects and their number

$$R = \left[ \Psi_{opt} / \Psi_{opt} \right] \times 100. \quad (14)$$

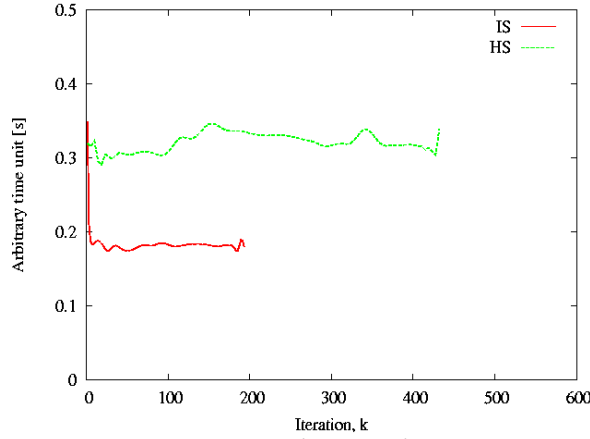


Figure 7, Comparison between the CPU times.

As far as the first test case, a square homogeneous host medium of size  $L_H = 0.8\lambda$  ( $d_{\max} = \sqrt{2}L_H$ ) characterized by a dielectric permittivity  $\varepsilon_H = 2.4$ , a conductivity  $\sigma_H = 2.4$ , and homogeneous defects ( $\varepsilon_{D_i} = 1.0, \sigma_{D_i} = 1.0$ ) has been considered. The samples of the scattered electric field have been collected at  $M=50$  equally-spaced measurement points located on a circle of radius  $\rho = 0.64\lambda$ .

Concerning the GA-based optimization, the following configuration of parameters has been adopted [10][11]:  $Q=80$ ,  $\pi_b = \pi_d = 0.7$ ,  $\pi_m = 0.4$  (mutation probability),  $C_{\max}=3$ ,  $K_{\max} = 600$ , and  $\Omega_{th} = 10^{-5}$ .

In order to evaluate the effectiveness of the multicrack strategies in dealing with single-crack detection (i.e., the single-crack techniques FGA [6] and IGA [7]), an unknown defect ( $C=1$ ) of area  $A_c / \lambda^2 = 2.25 \times 10^{-2}$  has been located at  $x_c / \lambda = 0.22$  and  $y_c / \lambda = 0.15$ . Moreover, the scattering data have been corrupted with different degree of noise (from  $SNR=5dB$  up to  $SNR=30dB$ ).

Figs. 1 and 2 show the values of the reconstruction errors obtained at the convergence. Due to the stochastic nature of the proposed approach, these results are the average values of the errors coming from 10 independent realization of the random process.

As far as the localization error is concerned (Fig. 1), the IGA-based approaches allow a non-negligible improvement in the estimation of the centers of the objects. As a matter of fact, an average error of 25% turns out for FGA, whereas IGA-based techniques provide a localization with an error lower than 20% also when  $SNR=5dB$ . Furthermore, IGA-based multicrack approaches overcome the IGA: when  $SNR < 12dB$ ,  $\delta_{IGA} > \delta_{IGA-HS} > \delta_{IGA-IS}$  in spite of the enlargement of the research space ( $C_{\max}=3$ ).

In the estimation of the area  $A_c$ , the performance achieved by the IS is comparable with that of single-crack approaches (Fig. 2), whereas the hierarchical approach does not reach the accuracy of single-crack algorithms.

The second test case is aimed at evaluating the detection of multiple crack. Towards this end, three geometries have been taken into account characterized by the presence of a number of cracks from  $C=1$  up to  $C=3$ . The positions and sizes of the cracks are reported in the following:

- $\{x_1 / \lambda, y_1 / \lambda, A_1 / \lambda^2\} = \{0.22, 0.15, 0.0225\}$
- $\{x_2 / \lambda, y_2 / \lambda, A_2 / \lambda^2\} = \{0.0; -0.15; 0.01\}$
- $\{x_3 / \lambda, y_3 / \lambda, A_3 / \lambda^2\} = \{-0.26; 0.15; 0.04\}$

The index  $R$  has been evaluated whatever the scattering scenario and in correspondence with different noise levels ( $SNR=10dB$ ,  $SNR=20dB$ ,  $SNR=30dB$ ). The resulting values are shown in Figs. 3 and 4. In general, the integrated strategy achieves better results with  $R > 90\%$ , except for the worst cases with  $SNR=10dB$ . On the contrary, HS reaches a value of precision recall smaller than the maximum value, with a lower resilience against noise than IS (e.g., in Fig. 3  $R \leq 40\%$  when  $SNR=10dB$ ).

As far as the reconstruction accuracy is concerned, the plots of the errors  $\delta$  and  $\Delta$  for  $C=\{2,3\}$  are shown in Figs. 5 and 6, respectively. For  $C=1$ , the error figures of IS and HS are shown in Figs. 1 and 2. The localizations of the defects are

performed with a satisfactory degree of accuracy for both techniques and for  $SNR > 15dB$  the centers of the defects are estimated with an error lower than 7%.

On the contrary, the estimation of the shape of the objects turns out to be quite difficult (Fig. 6). As a matter of fact, the error  $\Delta$  is lower than 60% for the integrated strategy, which overcomes the HS whatever the noise level and the value of  $C$ .

Finally, Fig. 7 deals with the computational cost of multicrack detection strategies. Once again, the IS turns out to be more effective than HS both in terms convergence rate and time per iteration.

#### 4. CONCLUSIONS

This paper deals with the detection of multiple scatterers in a known host medium. Starting from the inverse scattering equations, an integral formulation based on the definition of the inhomogeneous Green's function has been presented. Then, the arising problem has been addressed by means of two GA-based strategies exploiting the available a-priori information on the scenario under test.

The proposed numerical experimentations demonstrated that a satisfactory degree of accuracy in terms of localization and estimation of the size of defects can be reached. Moreover, the IS showed better results than HS, which is characterized by a lower convergence rate and higher computational costs.

#### 5. REFERENCES

1. R. Zoughi, *Microwave Nondestructive Testing and Evaluation*, Kluwer Academic Publishers, The Netherlands, 2000.
2. M. Tabib-Azar, "Applications of an ultra high resolution evanescent microwave imaging probe in the non-destructive testing of materials," *Materials Evolution*, vol. 59, pp. 70-78, 2001.
3. R. J. King and P. Stiles, "Microwave non-destructive evaluation of composites," *Review of Progress in Quantitative Nondestructive Evaluation*, vol. 3, pp. 1073-1081, Plenum, New York, 1984.
4. K. Belkebir, Ch. Pichot, J. Ch. Bolomey, P. Berthaud, G. Gottard, X. Derobert, and G. Fauchoux, "Microwave tomography system for reinforced concrete structures," *Proc. 24th European Microwave Conf.*, Cannes, France, pp. 1209-1214, 1994.
5. C. C. Chiu and P. T. Liu, "Image reconstruction of a perfectly conducting cylinder by the genetic algorithm," *IEE Proc. Microw. Antennas Propagat.*, vol. 3, p. 143, 1996.
6. S. Caorsi, A. Massa, and M. Pastorino, "A crack identification microwave procedure based on a genetic algorithm for nondestructive testing," *IEEE Trans. Antennas Propagat. Magazine*, vol. 37, pp. 7-15, 1995.
7. S. Caorsi, A. Massa, M. Pastorino, and M. Donelli, "Improved microwave imaging procedure for nondestructive evaluations of two-dimensional structures," *IEEE Trans. Antennas Propagat. Magazine*, vol. 39, no. 4, pp. 7-25, 1997.
8. S. Caorsi, G. L. Gragnani, M. Pastorino, and M. Rebagliati, "A model-driven approach to microwave diagnostics in biomedical applications," *IEEE Trans. Microwave Theory Tech.*, vol. 44, pp. 1910-1920, 1996.
9. J. H. Richmond, "Scattering by a dielectric cylinder of arbitrary cross-section shape," *IEEE Trans. Antennas Propagat.*, vol. AP-13, pp. 334-341, 1965.
10. R. L. Haupt and S. E. Haupt, *Practical Genetic Algorithm*, John Wiley & Sons Inc., New York, 1998.
11. J. M. Johnson and Y. Rahmat-Samii, "Genetic algorithms in engineering electromagnetics," *IEEE Trans. Antennas Propagat. Magaz.*, vol. 39, no. 4, pp. 7-25, 1997.